F. KAFEXHIU, F. VODOPIVEC, B. PODGORNIK

ISSN 0543-5846
METABK 56(3-4) 353-356 (2017)
UDC – UDK 669.15.26:536.45.42:620.18.17-536.5=111

ANALYSIS OF PRIMARY CREEP IN SIMULATED HEAT AFFECTED ZONE (HAZ) OF TWO 9 - 12 % Cr STEEL GRADES

Received – Prispjelo: 2017-01-04
Accepted – Prihvaćeno: 2017-04-25
Original Scientific Paper – Izvorni znanstveni rad

The primary creep of the parent metal (α), inter-critical (α+γ), and coarse-grained (γ) microstructures of simulated weld heat-affected zone (HAZ) for the steels X20CrMoV121 and X10CrMoVNb91, aged for 4 320 hours (6 months) at 750 °C and 17 520 hours (2 years) at 650 °C was analyzed. The time and creep strain at the transition point from primary to secondary creep were found to vary strongly between the parent metal and two simulated HAZ microstructures, especially after ageing at 750 °C.

Keywords: Martensitic 9-12 % Cr steels, ageing, microstructure, simulated HAZ, primary creep

INTRODUCTION

Creep resistant 9 - 12 % Cr steels are used in vital components of fossil-fired power plants, where operating parameters may reach up to 620 °C and 280 bar. Studies on creep resistance of such steels have been mainly focused on stationary (secondary) creep rate and rupture strength of parent metal. However, the weld heat affected zone (HAZ), a narrow zone of parent metal adjacent to the weld fusion line, is regarded as the most vulnerable failure location in respect to long-term creep strength [1]. In addition, the primary stage of accelerated creep test curve may provide valuable information on further course of the curve.

The purpose of the present work is to analyze the primary creep stage of the parent metal, inter-critical (α+γ), and coarse-grained (γ) microstructures of the simulated HAZ for two grades of 9 - 12 % Cr steels, i.e., the X20CrMoV121 (X20 hereafter) and X10CrMoVNb91 (P91 hereafter), after isothermal ageing of up to 4 320 hours (6 months) at 750 °C and 17 520 hours (2 years) at 650 °C.

EXPERIMENTAL

Chemical composition of the studied steels given in Table 1 was determined at the IMT using optical emission spectrometer with inductively coupled plasma.

Samples of both steels were austenitized at 1 050 °C, quenched in oil and tempered at 810 °C for 30 minutes. In this way, the microstructure of tempered martensite was obtained, which in our case is taken as the parent metal, from which the HAZ was simulated by additional heat treatments. The coarse-grained (γ) microstructure was obtained by keeping the samples at 1 000 °C (beyond Ac3) for 30 minutes, followed by air-cooling and tempering for additional 30 minutes at 740 °C – post weld heat treatment (PWHT). The inter-critical (α+γ) microstructure was obtained by keeping both samples at 845 °C (between Ac1 and Ac3) for 60 minutes, followed by air-cooling and the PWHT, as in the previous case.

Table 1 **Chemical composition of the steels X20 and P91 / wt. %**

Elements	X20	P91
C	0,20	0,10
Si	0,29	0,38
Mn	0,52	0,48
P	0,019	0,012
S	0,011	0,002
Cr	11,0	7,9
Ni	0,64	0,26
Mo	0,94	0,98
V	0,31	0,23
Cu	0,059	0,14
Nb	0,024	0,11
Al	0,032	0,016
N	0,017	0,064

In order to accelerate the microstructure changes that occur at service conditions, all samples were aged for 4 320 at 750 °C and up to 17 520 hours at 650 °C.

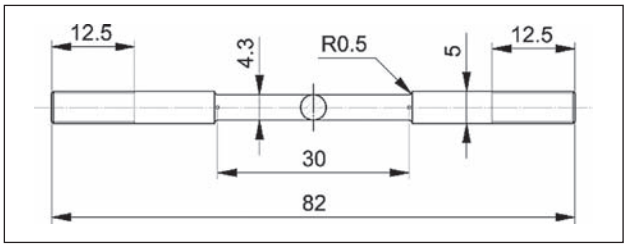

Figure 1 Creep test specimen

F. Kafexhiu, F. Vodopivec, B. Podgornik: Institute of metals and technology, Ljubljana, Slovenia.

The creep specimens (Figure 1) were prepared from the parent metal (α), simulated inter-critical (α+γ) and coarse-grained (γ) HAZ microstructures. Creep tests were performed at 170 MPa / 580 °C, lasting up to 100 h, with exceptions where specimens happened to rupture earlier.

Scanning electron microscopy (SEM) imaging was performed with the purpose of evaluating the microstructure evolution due to the ageing at 750 °C.

CURVE FITTING

Mathematical representation of creep curve has been a subject of interest in many articles [1]. In our case, the following expression, which is a modified form of the power law that represents the dependence of creep strain (ε) on time (*t*), given by Graham and Walles [2] was applied:

$$\varepsilon(t) = \mathrm{A} \cdot \sigma \cdot t^{\frac{\mathrm{B}}{T}} \tag{1}$$

with creep test parameters σ = 170 MPa and *T* = 853 K, and fitting parameters A and B. Equation (1) and Equation (2) (Norton-Bailey) [3] provide identical and better fitting with experimental data (Figure 8) as compared to Equation (3) (Garofalo) [4, 5].

$$\varepsilon_p(t) = d_1 \cdot \sigma^n \cdot t^p \tag{2}$$

$$\varepsilon(t) = \varepsilon_i + \varepsilon_{p1\max} \cdot \left(1 - e^{-D(t/t_{i2})^{\mu}}\right) \tag{3}$$

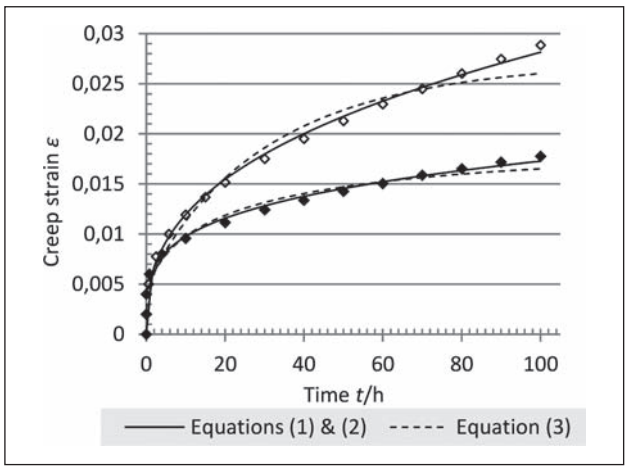

Figure 2 Primary creep curve fitting

RESULTS

Figure 3 shows the creep tests data and the corresponding fitted curves by Equation (1) for the parent metal (α), inter-critical (α+γ) and coarse-grained (γ) microstructures for both X20 and P91 steels at the initial state.

From Figure 3, it is evident that the steel P91 as compared to X20 shows higher creep resistance for half order of magnitude. This behavior is proportional for all three microstructures of both steels, where (γ) HAZ microstructure showed the highest creep resistance whereas (α+γ) the lowest.

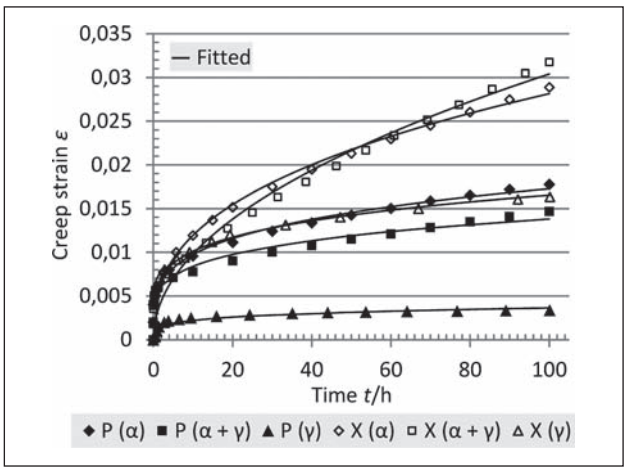

Figure 3 Primary creep of parent metal (α), simulated inter-critical (α+γ) and coarse-grained (γ) HAZ microstructures of the steels X20 and P91 at the initial state

Figure 4 shows the creep data and the corresponding fitted curves after ageing for 2 years at 650 °C. After 2 years of ageing at 650 °C, there is a small difference in creep behavior of three different microstructures of the steel P91, which performed better than the steel X20. (γ) microstructure of the steel X20 showed higher creep resistance as compared to the (α+γ) and (α), which already experience the ternary creep.

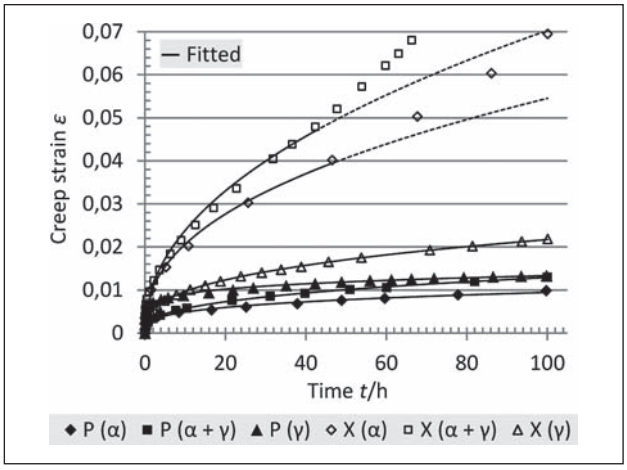

Figure 4 Primary creep of parent metal (α), simulated inter-critical (α+γ) and coarse-grained (γ) HAZ microstructures of the X20 and P91 steels, aged for 2 years at 650 °C

Figure 5 shows the creep data after ageing for 6 months at 750 °C. From Figure 5a it is evident that all three microstructures of both X20 and P91 steels have experienced the ternary creep stage and specimens ruptured in less than 60 h of creep test, at the best scenario. (α) and (γ) HAZ microstructures of the steel P91 showed the highest creep resistance, whereas the lowest was observed for (α+γ) and (γ) HAZ microstructures of the

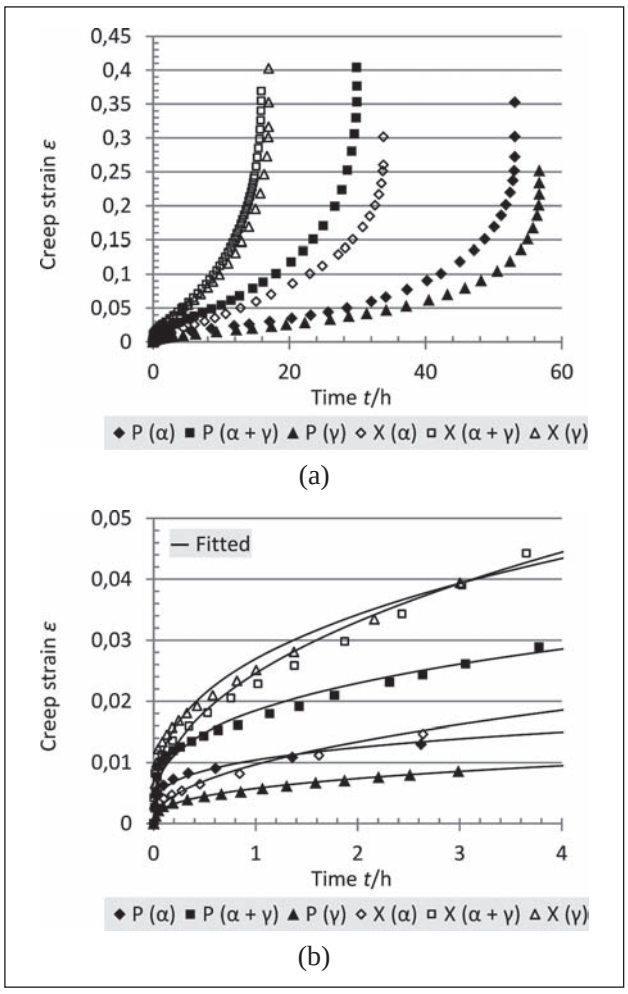

Figure 5 Primary creep of parent metal (α), simulated inter-critical (α+γ) and coarse-grained (γ) HAZ microstructures of the X20 and P91 steels, aged for 6 months at 750 °C; (b) in an enlarged part of (a)

steel X20. This behavior is also evident in the primary creep stage (Figure 5b), although not as clear as in Figure 5a.

SEM images in Figures 6 and 7 show the microstructure evolution of the simulated inter-critical (α+γ) and coarse-grained (γ) HAZ microstructures of the steel X20 after 6 months of ageing at 750 °C. For the steel P91, the respective evolution is shown by the SEM images in Figures 8 and 9.

From all SEM images above, it can be noticed that ageing at 750 °C caused the coarsening of carbide and

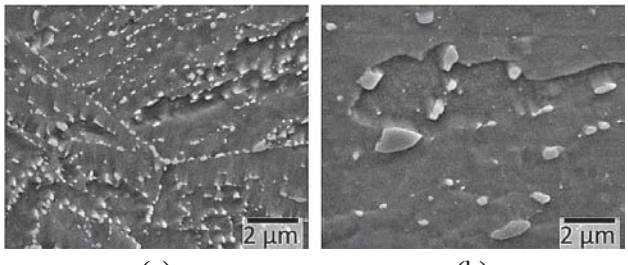

Figure 6 Evolution of the simulated (α+γ) HAZ microstructure of the steel X20; (a) initial state; (b) aged for 6 months at 750 °C

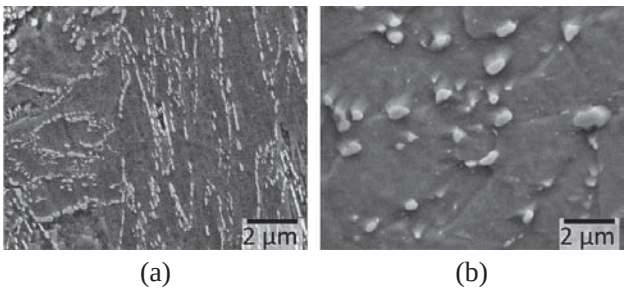

Figure 7 Evolution of the simulated (γ) HAZ microstructure of the steel X20; (a) initial state, (b) aged for 6 months at 750 °C

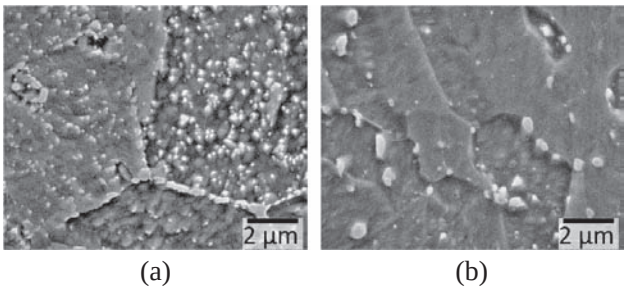

Figure 8 Evolution of the inter-critical (α+γ) microstructure of the steel P91; (a) initial state, (b) aged for 6 months at 750 °C

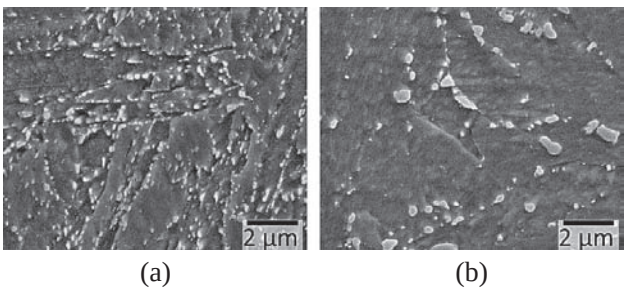

Figure 9 Evolution of the simulated (γ) HAZ microstructure of the steel P91; (a) initial state, (b) aged for 6 months at 750 °C

nitride particles and their redistribution from stringers along grain and subgrain boundaries to evenly distributed. In addition, the size and mutual spacing of precipitates increased, while the number density decreased correspondingly.

DISCUSSION

From creep curves in Figures 3, 4, and 5, it is obvious that ageing at 750 °C for 6 months has much greater effect on the creep behavior, as compared to the ageing at 650 °C for 2 years.

For the steel X20, it is obvious from Figures 3 and 4 that the simulated inter-critical (α+γ) HAZ microstructure has the highest creep strain, followed by the parent metal (α). These two microstructures experience another transition, i.e., from secondary to ternary creep after being aged at 650 °C for 2 years, in contrast to the simulated coarse-grained (γ) HAZ of the same steel and all three microstructures of the steel P91, which remained

at the secondary creep regime the whole 100 h of the creep test. From Figure 5a it is evident that all three microstructures of both X20 and P91 steels have experienced the ternary creep stage and specimens ruptured in less than 60 h of creep test, at the best scenario.

The effect of ageing is also expressed in the SEM images shown in Figures 6 - 9, with the special emphasis on coarsening, growth of mutual spacing, and redistribution of carbide and nitride precipitates, such as $M_{23}C_6$, VC, NbC, etc., as they have a great influence on the creep resistance of 9-12 % Cr steels [6]. The microstructure evolution after ageing at 750 °C is greater than the one after ageing at 650 °C, because of the highest diffusivity of carbide and nitride forming elements at higher temperatures. After 6 months of ageing at 750 °C, Figures 6 - 9 show the bigger greyish $M_{23}C_6$ particles, which grow faster because of high Cr content in the solid solution. In the steel X20, the small light precipitates (Figures 6 and 7) are of the VC type, whereas in the steel P91 (Figures 8 and 9), the VC and NbC precipitates are present, the latter being even more stable because of small content of Nb in solid solution [7].

Comparing the creep curves at the initial state and those after 6 months of ageing at 750 °C, with the microstructure evolution in SEM images (Figures 6 - 9), it can be noticed that there is a clear influence of both grain morphology and the size, distribution and mutual spacing of precipitates. It should be noted that, the mutual difference between different microstructures of both steels, and the difference between the steels X20 and P91 remains virtually the same after the ageing, i.e., due to ageing, the creep performance of all microstructures of both steels deteriorated proportionally as a function of tempering time and temperature.

Table 2 **Time and creep strain at the transition primary-secondary creep for X20 and P91 steels**

		Ageing	Transition time / h		Transition strain	
Steel	Microstructure	*t* / h / *T* / °C	0	17 520	0	17 520
				4 320		4 320
X20	α	650	60	27	0,023	0,031
		750		2,15		0,013
	α+γ	650	58	20,5	0,041	0,0319
		750		0,53		0,0205
	γ	650	54	66	0.014	0,0188
		750		1,2		0,0269
P91	α	650	68.7	49,7	0,06	0,0076
		750		3,4		0,014
	α+γ	650	45	47	0,011	0,0097
		750		1,8		0,021
	γ	650	62	68	0,003	0,0126
		750		3		0,0086

Regarding the primary creep behavior, Table 2 shows the time and the creep strain at the transition point from primary to secondary creep. At the initial state (prior to ageing), differences in transition time are not so obvious, except for the simulated inter-critical (α+γ) HAZ microstructure of the steel P91, where the transition appears after 45 hours of the creep test. The creep strain at the transition point was the greatest for the simulated inter-critical (α+γ) HAZ of the steel X20 and the lowest for the coarse-grained (γ) HAZ microstructure of the steel P91. Greater changes in the transition time were observed after ageing at 750 °C for 6 months, where most of the transitions from primary to secondary creep appeared in less than 3 hours of creep test.

CONCLUSIONS

Ageing at 750 °C for 6 months showed much greater effects on the microstructure and properties, as compared to the ageing for 2 years at 650 °C.

The simulated inter-critical (α+γ) HAZ microstructure exhibited the lowest creep resistance, especially after ageing at 750 °C.

A parametric power law was proposed, providing excellent fit with the experimental data.

REFERENCES

[1] F. Abe, T.U. Kern and R. Viswanathan, Creep-resistant steels, Woodhead Publishing, CRC Press, Cambridge, England, 2008.

[2] A. Graham, K.F.A. Walles, 'Relations between long and short time properties of commercial alloys', JIS 179(1955), 105-120.

[3] F.N. Norton, The Creep of Steel at High Temperature, McGraw-Hill, 1929.

[4] F. Garofalo, Fundamentals of Creep and Creep Rupture in Metals, New York, Macmillan, 1965.

[5] K.H. Kloos, J. Granacher and M. Monsees, Creep equations for heat resistant steels, Steel research 69(1998)11, 446-453.

[6] F. Vodopivec, M. Jenko, R. Celin, B. Žužek, D.A. Skobir, Creep resistance of microstructure of welds of creep resistant steels, Materials and Technology 45(2011)2, 139-143.

[7] F. Vodopivec, D.S. Petrovič, B. Žužek, M. Jenko, Coarsening rate of $M_{23}C_6$ and MC particles in high chromium creep resistant steel, Steel Research International 10(2013) 1002.

Note: The responsible proofreader for English language is Sabina Berisha, Ljubljana, Slovenia